

## Fine-structure-resolved laser-photodetachment electron spectroscopy of $\text{In}^-$

W. W. Williams, D. L. Carpenter, A. M. Covington, and J. S. Thompson

*Department of Physics and Chemical Physics Program, University of Nevada, Reno, Nevada 89557-0058*

T. J. Kvale

*Department of Physics and Astronomy, University of Toledo, Toledo, Ohio 43606-3390*

D. G. Seely

*Department of Physics, Albion College, Albion, Michigan 49224*

(Received 16 June 1998)

The electron affinity of indium has been measured using the laser-photodetachment electron spectroscopy technique. Fine-structure-resolved photoelectron kinetic energy spectra of  $\text{In}^-$  were analyzed and the electron affinity of  $\text{In}(^2P_{1/2})$  was determined to be  $0.404 \pm 0.009$  eV. The fine-structure splittings in the ground state of  $\text{In}^-(^3P_{0,1,2})$  were determined to be  $0.076 \pm 0.009$  eV ( $J=0 \rightarrow J=1$ ) and  $0.175 \pm 0.009$  eV ( $J=0 \rightarrow J=2$ ). This measurement is compared to several recent calculations of the electron affinity of indium. [S1050-2947(98)04611-3]

PACS number(s): 32.10.Hq, 32.80.Gc

A number of recent investigations have reported calculations and experimental measurements of the electron affinities of the group 13 elements. However, the column containing the group 13 elements is one of the few in the periodic table where experimental measurements of electron affinities are not available for comparison with calculations for all of the members of the group [1,2]. Theoretical investigations of electron affinities are difficult due to the importance of the treatment of electron correlation in the calculations. In general, as the atomic number  $Z$  of the negative ion species increases, calculations become more difficult due to the number of electrons that must be considered and the increasing importance of relativistic effects in the calculations. Therefore, it is important to test the validity of the predictions of the calculations with experimental measurements for each member in the group.

Boron, aluminum, and gallium are the only members of the group 13 elements for which electron affinities have been measured. The electron affinity of boron [279.723(25) meV] [3] was measured using the laser-photodetachment threshold technique. Two recent measurements of the electron affinities of aluminum and gallium have been reported. A very precise measurement of the electron affinity of aluminum [0.43283(5) eV] using tunable infrared laser spectroscopy was reported [4], and the electron affinity of gallium ( $0.43 \pm 0.03$  eV) was recently measured [5] using the laser photodetachment spectroscopy technique. The recommended value [1] for the electron affinity of indium ( $0.3 \pm 0.2$  eV) was determined using the results of a semiempirical extrapolation [6] and a photodetachment, relative cross-section measurement [7] that was unable to reach the energy threshold for photodetaching  $\text{In}^-$ .

Several recent theoretical investigations of the electron affinity of indium, using different techniques, have reported calculations of the electron affinity of indium. Guo and Whitehead [8], in a study of the ionization potentials and electron affinities of high- $Z$  atoms, used a generalized-exchange local-spin-density-functional theory with a self-

interaction correction [9] to calculate the electron affinity of indium as 0.371 eV. Arnau *et al.* [10] used a form of the multireference single- and double-configuration interaction method to predict the electron affinity of indium to be 0.38 eV. Wijesundera [11] predicted the electron affinity of  $\text{In}(^2P_{1/2})$  to be 0.393 eV using the multiconfiguration Dirac-Fock method. Also, Eliav *et al.* predicted the electron affinity of indium to be 0.419 eV using a relativistic coupled-cluster method [12].

In this paper, we report an experimental determination of the electron affinity of indium. The measurements were made using the laser-photodetachment spectrometry technique. A detailed description of the experimental apparatus has been given previously [13,14], but a brief description follows. Negative ions used in the experiment were produced with a cesium-sputter negative ion source. In this ion source, energetic  $\text{Cs}^+$  ions (3 keV) were accelerated and focused onto a target, where negative ions were sputtered from the target material. The target for this experiment was a pressed pellet of  $\text{In}_2\text{O}_3$ ,  $\text{Na}_2\text{CO}_3$ , and Cu powders. The negative ions were extracted from the ion source by applying a bias voltage of  $-10$  kV to the ion source, which accelerated the negative ions toward ground potential. The extracted negative ion beam was focused onto the entrance slit of a  $90^\circ$ , double-focusing, bending magnet that momentum selected the negative ion beam for the experiment. The mass resolution of the bending magnet was approximately 1:200 ( $\Delta m/m$ ), thereby ensuring that an isotopically pure indium negative ion beam was directed into the interaction chamber. The  $^{115}\text{In}^-$  beam was identified in the mass scan by locating the copper dimer anions and the isotopes of tin anions also emitted from the negative ion source. The pressure in the beam line was on the order of  $1 \times 10^{-6}$  Pa and the total flight length of the beam line was 6.4 m.

After entering the experimental chamber, the negative ion beam was crossed at  $90^\circ$  with a linearly polarized photon beam produced by a 25-W argon ion laser. Photon wavelengths of 514.5 nm (2.41 eV) and 488.0 nm (2.54 eV) were

used in these experiments. The photon beam traversed a Glan-laser polarizer and a double-Fresnel rhomb ( $\lambda/2$  phase retarder) before crossing the negative ion beam. The polarizer set the linear polarization of the laser light with an extinction ratio of at least  $10^5$  to 1 and the double Fresnel rhomb was used to rotate the linear polarization vector of the light. The laser beam was monitored with a thermopile power meter following the crossing of the ion and laser beams. Typical laser powers were 7.0 W at 514.5 nm and 5.0 W at 488.0 nm.

Photodetached electrons were energy analyzed with an electrostatic  $160^\circ$  spherical-sector spectrometer and detected with a channel-electron multiplier. The electron energy analyzer was operated in the constant pass energy mode. A bias voltage was applied to the analyzer to accelerate the photoelectrons to a determined kinetic energy that permitted the acquisition of electron kinetic energy spectra. The entrance aperture of the spectrometer was located at  $45^\circ$  relative to the ion beam velocity vector and in the plane perpendicular to the plane containing the ion and photon beams. The ion and laser beams crossed approximately 2.5 cm from the entrance aperture to the spectrometer. The spectrometer and the photon-negative ion interaction region were enclosed in a mu-metal box, and a set of mutually perpendicular coils enclosed the experimental chamber to reduce the intensity of the Earth's and stray magnetic fields in the experimental chamber. Typical pressure in the experimental chamber was  $2 \times 10^{-7}$  Pa. The ion beam intensity was monitored with an electrometer connected to a Faraday cup in the experimental chamber. Voltage output signals from both the laser power meter and the electrometer were digitized with voltage-to-frequency converters and recorded for normalization of the electron signal.

A typical photoelectron kinetic energy spectrum for  $\text{In}^-$  is shown in Fig. 1. The kinetic energy of the  $\text{In}^-$  ions in the beam was 10 keV for this spectrum, and the ion current measured in the experimental chamber was approximately 1 nA. The photon wavelength was 514.5 nm and the power of the photon beam was 6 W. The double-Fresnel rhomb was set so the polarization vector of the laser light pointed toward the entrance aperture of the electron spectrometer for this particular spectrum. The data accumulation time for each data point was 60 s and the spectrum took approximately 50 min to complete. The data points are plotted with error bars that represent their uncertainty due to counting statistics at one standard deviation. The solid line represents a weighted least-squares fit to six Gaussian functions with a linear background.

The energy scale for the  $\text{In}^-$  photoelectron kinetic energy spectra was determined using the photoelectron energy spectra of  $\text{Na}^-$ . Photoelectron kinetic energy spectra of  $\text{Na}^-$  were taken with either 488.0 nm or 514.5 nm laser light before and after each  $\text{In}^-$  photoelectron energy spectrum was collected. The electron affinity of Na [0.547 9309(25) eV] was precisely determined by a laser photodetachment threshold experiment [1]. Typical signal-to-noise ratios for the present photoelectron kinetic energy spectra of  $\text{Na}^-$  were 20:1. The technique for determining the energy scale for the  $\text{In}^-$  photoelectron energy scale is described as follows. The

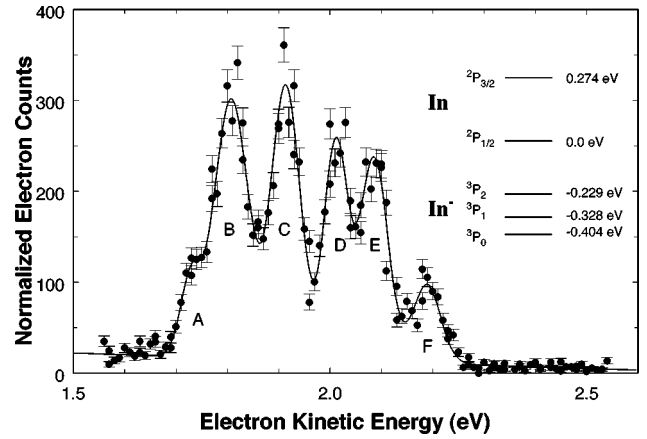


FIG. 1. Typical photoelectron kinetic energy spectrum for photodetaching  $\text{In}^-$ . The ion beam energy was 10 keV and the photon wavelength was 514.5 nm (2.410 eV) for this spectrum. The data points are plotted with error bars representing counting statistics at one standard deviation. The solid line is a nonlinear least-squares fit to the data with six Gaussian functions and a linear background. Prominent features in the photoelectron spectrum resulting from the photodetachment of  $\text{In}^-$  are labeled A–F and are identified in the text. The energy levels of  $\text{In}^-$  and  $\text{In}$  corresponding to the six photoelectron peaks are shown in the accompanying energy-level diagram. The electron affinity of indium is the energy difference between the  $\text{In}(^2P_{1/2})$  and  $\text{In}^-(^3P_0)$  levels.

kinetic energy of the photoelectrons from the reference ion, as measured in the laboratory frame, was determined using the equation

$$E_l = (\sqrt{\epsilon} \cos \theta_l + \sqrt{E_c - \epsilon \sin^2 \theta_l})^2, \quad (1)$$

where  $E_l$  is the laboratory frame energy of the photoelectrons, and  $\theta_l$  is the angle between the velocity vector of an ion in the beam and the collection direction for the photoelectrons ( $45^\circ$  for this experiment). The term  $\epsilon$  is the kinetic energy of an electron with the same velocity as the ions in the beam, i.e.,  $\epsilon = (m_e/m_i)E$ , where  $m_e$  and  $m_i$  are the masses of an electron and an ion in the beam, respectively, and  $E$  is the kinetic energy of an ion in the beam.  $E_c$  is the kinetic energy of the photodetached electrons in the rest frame of the ion and is given by  $E_c = E_\gamma - E_a$ , where  $E_\gamma$  is the photon energy and  $E_a$  is the electron affinity associated with the Na reference atom. The laboratory frame energy,  $E_l$ , for photoelectrons from the reference ions was determined using Eq. (1). The value of the energy centroid of the  $\text{Na}^-$  reference ion photoelectron peak was determined using a weighted least-squares fit to a Gaussian function with a linear background. The fitted value of the energy centroid was then assigned the value of  $E_l$  for photoelectrons from the reference ion for the experimental conditions.

The energy scale for the  $\text{In}^-$  photoelectron spectra in the laboratory frame was then referenced to  $\text{Na}^-$  photoelectron spectra. The  $\text{In}^-$  photoelectron spectra were then transformed into the rest frame of the indium anion using the formula

$$E_c = E_l + \epsilon - 2\sqrt{\epsilon E_l} \cos \theta_l, \quad (2)$$

where  $E_c$  is the energy of the photoelectrons resulting from photodetachment of  $\text{In}^-$  in the ion rest frame. The electron affinity of indium was then determined using the equation  $E_c = E_\gamma - E_a$ .

Six photoelectron peaks were observed in the photoelectron kinetic energy spectra for  $\text{In}^-$  and are labeled A–F in Fig. 1. The six peaks correspond to the photodetachment channels due to the energy splitting of the fine-structure levels in the process  $h\nu + \text{In}^-(^3P_{0,1,2}) \rightarrow \text{In}(^2P_{1/2,3/2}) + e^-$ . The energy separation of the fine structure levels in the ground state of  $\text{In}(^2P_{1/2,3/2})$  is well known (0.274 eV) [15], and was used in the analysis of the photodetachment data. The six peaks in the spectra were fitted to Gaussian functions with a linear background using a weighted least-squares fit to determine their energy centroids. The three higher-energy photoelectron peaks (D, E, and F) were due to photodetachment into the  $^2P_{1/2}$  level of indium (peak F was due to the photodetachment channel  $^3P_2 \rightarrow ^2P_{1/2}$ ; peak E was due to the photodetachment channel  $^3P_1 \rightarrow ^2P_{1/2}$ ; and peak D was due to the photodetachment channel  $^3P_0 \rightarrow ^2P_{1/2}$ ). The three lower-energy photoelectron peaks (A, B, and C) were a result of photodetachment into the  $^2P_{3/2}$  level of indium (peak C was due to the photodetachment channel  $^3P_2 \rightarrow ^2P_{3/2}$ ; peak B was due to the photodetachment channel  $^3P_1 \rightarrow ^2P_{3/2}$ ; and peak A was due to the photodetachment channel  $^3P_0 \rightarrow ^2P_{3/2}$ ). The photoelectron peak labeled D at  $\sim 2.0$  eV was due to the photodetachment channel  $h\nu + \text{In}^-(^3P_0) \rightarrow \text{In}(^2P_{1/2}) + e^-$ , which is the ground-state negative ion to ground-state atom transition, and was used to determine the electron affinity of indium. The fine-structure splitting in  $\text{In}^-(^3P_{0,1,2})$  was also determined from the spectra, using the known fine-structure splitting in  $\text{In}(^2P_{1/2,3/2})$  [15]. The relative intensities of the six photoelectron peaks in the spectrum were a result of the initial-state populations of the fine-structure levels of  $\text{In}^-$ , the relative probabilities of the observed photodetachment channels, and the photoelectron angular distributions of each photodetachment channel, and

were not investigated for this study. No other peaks were observed in the  $\text{In}^-$  photoelectron spectra, since the first excited state in indium lies 3.02 eV above the ground state [15] of indium.

Twelve photoelectron spectra of  $\text{In}^-$  were collected and reference photoelectron spectra of  $\text{Na}^-$  were collected before and after each  $\text{In}^-$  spectrum. This technique yielded the electron affinity of  $\text{In}(^2P_{1/2})$  to be  $0.404 \pm 0.009$  eV. The fine-structure splittings in the ground state of  $\text{In}^-$  were determined as  $0.076 \pm 0.009$  eV ( $J=0 \rightarrow J=1$ ) and  $0.175 \pm 0.009$  eV ( $J=0 \rightarrow J=2$ ). The total uncertainty in the electron affinity and fine-structure splitting measurements is reported at one standard deviation. Included in the total uncertainty were the uncertainties in the electron affinities of the reference ion, the uncertainty in determining the ion beam energy, and the uncertainty in determining the energy centroid of the photoelectron peaks in the spectra.

The measured electron affinity of  $\text{In}(^2P_{1/2})$ ,  $0.404 \pm 0.009$  eV, is in excellent agreement with the previously reported calculations [8,10,12,11] and in good agreement with the recommended value,  $0.3 \pm 0.2$  eV, of Hotop and Lineberger [1]. The measured fine-structure splittings in the ground state of  $\text{In}^-$ ,  $0.076 \pm 0.009$  eV ( $J=0 \rightarrow J=1$ ) and  $0.175 \pm 0.009$  eV ( $J=0 \rightarrow J=2$ ) are in good agreement with recommended values ( $0.084 \pm 0.009$  eV and  $0.192 \pm 0.019$  eV, respectively) [1], which were determined by isoelectronic extrapolation. Future investigations of the electron affinity of thallium are planned so that a complete set of experimentally determined electron affinities of the group 13 elements will be available for comparison with theoretical predictions.

This work was supported by the National Science Foundation under Cooperative Agreement No. OSR-935227. T.J.K. acknowledges support from a grant from the Division of Chemical Sciences, Office of Basic Energy Sciences, Office of Energy Research of the U.S. Department of Energy. D.G.S. acknowledges support from Albion College.

- 
- [1] H. Hotop and W. C. Lineberger, *J. Phys. Chem. Ref. Data* **14**, 731 (1985).
- [2] *Handbook of Chemistry and Physics*, edited by David R. Lide (CRC Press, Boca Raton, FL, 1997), Vol. 78, pp. 10–187.
- [3] Michael Scheer, René C. Bilodeau, and Harold K. Haugen, *Phys. Rev. Lett.* **80**, 2562 (1998).
- [4] Michael Scheer, René C. Bilodeau, Jan Thøgersen, and Harold K. Haugen, *Phys. Rev. A* **57**, R1493 (1998).
- [5] W. W. Williams, D. L. Carpenter, A. M. Covington, M. C. Koepnick, D. Calabrese, and J. S. Thompson, *J. Phys. B* **31**, L341 (1998).
- [6] R. J. Zollweg, *J. Chem. Phys. Lett.* **50**, 4251 (1969).
- [7] D. Feldman, R. Rackwitz, E. Heinicke, and H. J. Kaiser, *Z. Naturforsch. A* **32**, 302 (1977).
- [8] Yufei Guo and M. A. Whitehead, *Phys. Rev. A* **38**, 3166 (1988).
- [9] S. H. Vosko, L. Wilk, and M. Nusair, *Can. J. Phys.* **58**, 1200 (1980).
- [10] Arnau Ferran, Fernando Moto, and Juan Novoa, *Chem. Phys.* **166**, 77 (1992).
- [11] W. P. Wijesundera, *Phys. Rev. A* **55**, 1785 (1997).
- [12] Ephraim Eliav, Yasyuli Ishikawa, Pekka Pykkö, and Uzi Kaldor, *Phys. Rev. A* **56**, 4532 (1997).
- [13] A. M. Covington, D. Calabrese, W. W. Williams, J. S. Thompson, and T. J. Kvale, *Phys. Rev. A* **56**, 4746 (1997).
- [14] D. Calabrese, A. M. Covington, D. L. Carpenter, J. S. Thompson, T. J. Kvale, and R. L. Collier, *J. Phys. B* **30**, 4791 (1997).
- [15] *Atomic Energy Levels Vol. III*, edited by Charlotte E. Moore, Natl. Bur. Stand. (U.S.) Circ. No. 467 (U.S. GPO, Washington, DC, 1952), p. 130.